Characteristic Mode Formulation for Dielectric Coated Conducting Bodies

Liwen Guo, Yikai Chen, *Senior Member, IEEE*, and Shiwen Yang, *Senior Member, IEEE*

***Abstract*— In this paper, characteristic mode (CM) formulations are developed from surface integral equation (SIE) for the modal analysis of dielectric coated conducting bodies. The electric field integral equation-Poggio, Miller, Chang, Harrington, Wu, and Tsai SIE is used for modeling the dielectric coated conducting bodies. By ensuring the field continuity on the interface boundary, two types of generalized eigenvalues equations are formulated to determine the resonant behavior of the dielectric coated conducting bodies. Following Poynting's theorem, the resultant eigenvalues indicate the ratio of the imaginary and real part of the complex power for each CM. Zero eigenvalues indicate the resonance in dielectric coated conducting bodies. The corresponding modal fields provide with clear physical insights into the radiation/scattering mechanisms. Numerical results are presented to demonstrate the accuracy of the proposed CM formulations.**

***Index Terms*— Characteristic modes (CMs), dielectric coated conducting bodies, electric field integral equation (EFIE)-Poggio, Miller, Chang, Harrington, Wu, and Tsai (PMCHWT), surface integral equation (SIE).**

I. Introduction

ELECTROMAGNETIC (EM) radiation/scattering from dielectric coated conducting bodies has been extensively studied [5]–[10]. For canonical dielectric coated conducting bodies, the scattering response can be readily obtained from Mie series [5], [6]. Modal analysis for such canonical problems is also available with the using of analytical methods [7]. For more general dielectric coated conducting bodies, EM numerical techniques, including integral equation methods and differential equation methods, are usually required [8]–[10]. It is observed that the scattering responses and radiation performance of dielectric coated conducting bodies heavily depend on external excitations or EM sources. However, the conventional EM numerical techniques, such as the method of moments (MoM) and the finite-element method, provide with little physical insight into the scattering or radiation mechanisms.

Garbacz [1] proposed the theory of characteristic modes (CMs) to determine the modal currents and modal fields for perfectly electrically conducting (PEC) bodies. It offers deep physical insights into various antenna designs [27] as well as scattering analysis and synthesis [11]–[14]. Harrington and Mautz [2] reformulated the CM theory by implementing the MoM in the electric field integral equation (EFIE). This CM formulation for PEC bodies has found wide applications in a variety of antenna designs, including platform integrated antenna system designs [18]–[21], multiple-input multiple-output antenna designs [22]–[24], and antenna array designs [25], [26]. Harrington *et al.* [3] has also extended the CM theory for the modal analysis of material bodies by using the volume integral equation [3] and surface integral equation (SIE) [4], respectively. Very recently, CM formulations for the modal analysis of material bodies have been further addressed in [15]–[17]. In [15], a novel CM formulation using the Poggio, Miller, Chang, Harrington, Wu, and Tsai (PMCHWT) equations was proposed. It allowed accurate prediction of the resonant frequencies and provided with accurate modal fields for arbitrarily shaped dielectric bodies. CM theory for material bodies was also formulated using the finite-element boundary-integral method [16]. In [17], a postprocessing method was proposed to remove the internal resonances. It was demonstrated to be capable of providing unique and real characteristic for material bodies.

The goal of this paper is to extend the theory of CMs from simple PEC bodies or material bodies to dielectric coated conducting bodies. This is also a natural extension as the merits of CM theories have been well recognized in our EM community and modal analysis for antennas with composite structures is becoming more necessary for performing systematic designs. Starting from the EFIE-PMCHWT SIE, the CM formulations are rigorously derived in Section II. In Section III, numerical results are then provided to demonstrate the accuracy of the proposed CM formulations. Final conclusions are presented in Section IV.

II. CM Theory for Dielectric Coated Conducting Bodies

A. EFIE-PMCHWT Formulation

Fig. 1 shows the configuration of a dielectric coated conducting body immersed in a background medium with medium parameters (ε_1, μ_1). The conducting body is fully coated by a material with medium parameters (ε_2, μ_2). The surfaces of the conducting body and the dielectric coatings are denoted by S_c and S_d, respectively. The region of the homogeneous background is denoted by V_1 and the volume of the dielectric coatings is denoted by V_2. $\hat{n}$ is the outward normal unit vector. We assume the dielectric coated conducting body is illuminated by an incident plane wave ($\mathbf{E}^i$, $\mathbf{H}^i$).

By applying the equivalence principle, the original problem can be described by considering its two equivalent

Manuscript received August 20, 2016; revised November 23, 2016; accepted December 9, 2016. Date of publication January 4, 2017; date of current version March 1, 2017. This work was supported by the Natural Science Foundation of China under Grant 61671127 and Grant 61631006. *(Corresponding author: Yikai Chen.)*

The authors are with the School of Electronic Engineering, University of Electronic Science and Technology of China, Chengdu 611731, China (e-mail: ykchen@uestc.edu.cn).

Color versions of one or more of the figures in this paper are available online at http://ieeexplore.ieee.org.

Digital Object Identifier 10.1109/TAP.2016.2647687

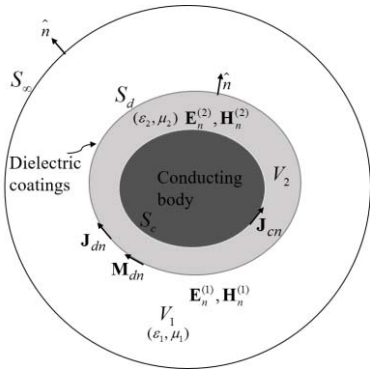

Fig. 1. Configuration of a dielectric coated conducting body.

problems [8]. It can be formulated in terms of the equivalent surface electric current $\mathbf{J}_c$ on the conducting surface S_c, the electric current $\mathbf{J}_d$, and magnetic current $\mathbf{M}_d$ on the dielectric surface S_d. The equivalent surface currents satisfy the following EFIE-PMCHWT formulations [8]:

$$\left[\eta_2 \mathcal{L}_2^c(\mathbf{J}_c) - \eta_2 \mathcal{L}_2^d(\mathbf{J}_d) - \mathcal{K}_2^d(\mathbf{M}_d)\right]_{\tan} = 0 \text{ on } S_c \tag{1}$$

$$\begin{bmatrix} \eta_2 \mathcal{L}_2^c(\mathbf{J}_c) - \eta_1 \mathcal{L}_1^d(\mathbf{J}_d) - \eta_2 \mathcal{L}_2^d(\mathbf{J}_d) \\ -\mathcal{K}_1^d(\mathbf{M}_d) - \mathcal{K}_2^d(\mathbf{M}_d) \end{bmatrix}_{\tan} = \mathbf{E}^i_{\tan} \text{ on } S_d \tag{2}$$

$$\begin{bmatrix} -\mathcal{K}_2^c(\mathbf{J}_c) + \mathcal{K}_1^d(\mathbf{J}_d) + \mathcal{K}_2^d(\mathbf{J}_d) \\ -\frac{1}{\eta_1}\mathcal{L}_1^d(\mathbf{M}_d) - \frac{1}{\eta_2}\mathcal{L}_2^d(\mathbf{M}_d) \end{bmatrix}_{\tan} = \mathbf{H}^i_{\tan} \text{ on } S_d \tag{3}$$

where the subscript "tan" refers to the tangential component of the fields, and $\eta_i = (\mu_i/\varepsilon_i)^{1/2}$ is the intrinsic wave impedance in region V_i. The operators $\mathcal{L}_i^v$ and K_i^v are given by [29]

$$\mathcal{L}_i^v(\mathbf{X}) = jk_i \oint_{S_v} \left[\mathbf{X}(\mathbf{r}')G_i(\mathbf{r},\mathbf{r}') + \frac{1}{k_i^2}\nabla' \cdot \mathbf{X}(\mathbf{r}')\nabla G_i(\mathbf{r},\mathbf{r}')\right] dS_v' \tag{4}$$

$$\mathcal{K}_i^v(\mathbf{X}) = P.V. \oint_{S_v} \mathbf{X}(\mathbf{r}') \times \nabla G_i(\mathbf{r},\mathbf{r}') dS_v' \tag{5}$$

where k_i is the wavenumber in region V_i, $G_i(\mathbf{r},\mathbf{r}')$ is the Green's function in an unbounded homogeneous medium with the constitutive parameters (ε_i, μ_i), and v denotes the surface that the source point $\mathbf{r}'$ resides on. *P.V.* represents the Cauchy principal value of the integration.

Applying Rao-Wilton-Glisson (RWG) basis functions $\mathbf{f}_l$ to expand the equivalent currents and testing the integral equations (1)–(3) using the same set of bases $\mathbf{f}_k$, it gives the following matrix equations:

$$Z_c^{\mathrm{EJ}_c} J_c + Z_c^{\mathrm{EJ}_d} J_d + Z_c^{\mathrm{EM}_d} M_d = 0 \tag{6}$$

$$Z_d^{\mathrm{EJ}_c} J_c + Z_d^{\mathrm{EJ}_d} J_d + Z_d^{\mathrm{EM}_d} M_d = V^E \tag{7}$$

$$Z_d^{\mathrm{HJ}_c} J_c + Z_d^{\mathrm{HJ}_d} J_d + Z_d^{\mathrm{HM}_d} M_d = V^H \tag{8}$$

where the elements in the submatrices and vectors are given by

$$\left[Z_c^{\mathrm{EJ}_c}\right]_{kl} = \eta_2 \oint_{S_c} \mathbf{f}_k \cdot \mathcal{L}_2^c(\mathbf{f}_l) dS_c \tag{9}$$

$$\left[Z_c^{\mathrm{EJ}_d}\right]_{kl} = -\eta_2 \oint_{S_c} \mathbf{f}_k \cdot \mathcal{L}_2^d(\mathbf{f}_l) dS_c \tag{10}$$

$$\left[Z_c^{\mathrm{EM}_d}\right]_{kl} = -\oint_{S_c} \mathbf{f}_k \cdot \mathcal{K}_2^d(\mathbf{f}_l) dS_c \tag{11}$$

$$\left[Z_d^{\mathrm{EJ}_c}\right]_{kl} = \eta_2 \oint_{S_d} \mathbf{f}_k \cdot \mathcal{L}_2^c(\mathbf{f}_l) dS_d \tag{12}$$

$$\left[Z_d^{\mathrm{EJ}_d}\right]_{kl} = -\eta_1 \oint_{S_d} \mathbf{f}_k \cdot \mathcal{L}_1^d(\mathbf{f}_l) dS_d - \eta_2 \oint_{S_d} \mathbf{f}_k \cdot \mathcal{L}_2^d(\mathbf{f}_l) dS_d \tag{13}$$

$$\left[Z_d^{\mathrm{EM}_d}\right]_{kl} = -\oint_{S_d} \mathbf{f}_k \cdot \mathcal{K}_1^d(\mathbf{f}_l) dS_d - \oint_{S_d} \mathbf{f}_k \cdot \mathcal{K}_2^d(\mathbf{f}_l) dS_d \tag{14}$$

$$\left[Z_d^{\mathrm{HJ}_c}\right]_{kl} = -\oint_{S_d} \mathbf{f}_k \cdot \mathcal{K}_2^c(\mathbf{f}_l) dS_d \tag{15}$$

$$\left[Z_d^{\mathrm{HJ}_d}\right]_{kl} = \oint_{S_d} \mathbf{f}_k \cdot \mathcal{K}_1^d(\mathbf{f}_l) dS_d + \oint_{S_d} \mathbf{f}_k \cdot \mathcal{K}_2^d(\mathbf{f}_l) dS_d \tag{16}$$

$$\left[Z_d^{\mathrm{HM}_d}\right]_{kl} = -\frac{1}{\eta_1} \oint_{S_d} \mathbf{f}_k \cdot \mathcal{L}_1^d(\mathbf{f}_l) dS_d - \frac{1}{\eta_2} \oint_{S_d} \mathbf{f}_k \cdot \mathcal{L}_2^d(\mathbf{f}_l) dS_d \tag{17}$$

$$[V^E]_k = \oint_{S_d} \mathbf{f}_k \cdot \mathbf{E}^i dS_d \tag{18}$$

$$[V^H]_k = \oint_{S_d} \mathbf{f}_k \cdot \mathbf{H}^i dS_d. \tag{19}$$

B. Definitions of Characteristic Currents and Characteristic Fields

Before proceeding to the theory of CMs for dielectric coated conducting bodies, we first clarify two points.

1) In the CM theory for dielectric coated conducting bodies, we intend to solve the equivalent surface electric currents on the conducting surface S_c, which will illustrate the modal behavior of the dielectric coated conducting bodies. Therefore, although the CM formulations are developed in terms of single current, i.e., the equivalent surface electric currents or the equivalent surface magnetic currents on the dielectric coating surface S_d, the equivalent surface electric currents on the conducting surface S_c will be eventually solved in both of the two CM formulations.
2) Similar to the CM theory for PEC bodies [2], the impressed field ($\mathbf{E}^i$, $\mathbf{H}^i$) is only defined in scattering problems for further CM theory derivations. No actual external source is considered in CM analysis problems. It indicates that the characteristic fields and characteristic currents in the CM theory for dielectric coated conducting bodies exist in a source-free problem.

Based on the above-mentioned important descriptions, we define $\mathbf{J}_{\mathrm{dn}}$ and $\mathbf{M}_{\mathrm{dn}}$ as the characteristic equivalent surface currents on the surface of the dielectric coatings, and define

$\mathbf{J}_{\rm cn}$ as the characteristic electric currents on the conducting surface (shown in Fig. 1). The subscript n denotes the order of the CMs and is numerically sorted by the absolute value of the eigenvalues. Moreover, $\mathbf{E}_n^{(i)}$ and $\mathbf{H}_n^{(i)}$ are defined as the characteristic electric fields and characteristic magnetic fields in region V_i generated by the characteristic currents. They are also shown in Fig. 1. Following the boundary conditions on S_c and S_d, it is easy to obtain the matrix equations that relate the characteristic currents and the characteristic fields:

$$Z_c^{\mathrm{EJ}_c} J_{\rm cn} + Z_c^{\mathrm{EJ}_d} J_{\rm dn} + Z_c^{\mathrm{EM}_d} M_{\rm dn} = V_{\rm pec}^E = 0 \text{ on } S_c \quad (20)$$

$$Z_d^{\mathrm{EJ}_c} J_{\rm cn} + Z_d^{\mathrm{EJ}_d} J_{\rm dn} + Z_d^{\mathrm{EM}_d} M_{\rm dn} = V_{\rm die}^E \text{ on } S_d \quad (21)$$

$$Z_d^{\mathrm{HJ}_c} J_{\rm cn} + Z_d^{\mathrm{HJ}_d} J_{\rm dn} + Z_d^{\mathrm{HM}_d} M_{\rm dn} = V_{\rm die}^H \text{ on } S_d \quad (22)$$

where $J_{\rm cn}$, $J_{\rm dn}$, and $M_{\rm dn}$ are the expansion coefficients of the RWG basis function for the characteristic surface currents $\mathbf{J}_{\rm cn}$, $\mathbf{J}_{\rm dn}$, and $\mathbf{M}_{\rm dn}$, respectively. $V_{\rm pec}^E$, $V_{\rm die}^E$, and $V_{\rm die}^H$ are vectors obtained by testing the characteristic fields using the RWG testing function $\mathbf{f}_k$, and the kth element of these vectors is given by

$$\left[V_{\rm pec}^E\right]_k = -\oint_{S_c} \mathbf{f}_k \cdot \left(\mathbf{E}_n^{(2)}\right)_{\tan} dS_c \quad (k = 1, 2 \ldots N_c) \quad (23)$$

$$\left[V_{\rm die}^E\right]_k = -\oint_{S_d} \mathbf{f}_k \cdot \left(\mathbf{E}_n^{(1)} - \mathbf{E}_n^{(2)}\right)_{\tan} dS_d \quad (k = 1, 2 \ldots N_d) \quad (24)$$

$$\left[V_{\rm die}^H\right]_k = -\oint_{S_d} \mathbf{f}_k \cdot \left(\mathbf{H}_n^{(1)} - \mathbf{H}_n^{(2)}\right)_{\tan} dS_d \quad (k = 1, 2 \ldots N_d) \quad (25)$$

where N_c and N_d are the numbers of basis functions on S_c and S_d, respectively.

Because the tangential component of the electric field over the conducting surface keeps zero, (20) is naturally satisfied and possesses clear physical meanings. In (21) and (22), it is necessary to properly enforce additional constrains to ensure the characteristic currents over the dielectric coating surfaces have physical meanings. When the tangential continuity of both E-field and H-field is imposed, i.e., the right-hand sides of (21) and (22) both equal to zero, the resultant resonance frequencies are complex numbers, and the modes solved are equivalent to the modes as defined in [30] and [31]. As compared with the methods in [30] and [31], one of the most attractive merits of the CM theory (including that for PEC bodies) is that it allows obtaining real resonant frequencies through sweeping along the real frequency axis. It greatly improves the computational efficiency in modal analysis over a wide frequency band. Therefore, to keep this natural merit in our proposed CM formulations for dielectric coated conducting bodies, two generalized eigenvalue equations are defined by enforcing different field continuity conditions.

C. Electric Field Continuity

Let the right-hand side of (21) equals to zero, it ensures the electric fields tangential continuity across the interface between regions V_1 and V_2. For convenience, let us first define two matrices

$$Z_{\rm mul}^A = \left[Z_c^{\mathrm{EJ}_c} - Z_c^{\mathrm{EJ}_d}\left(Z_d^{\mathrm{EJ}_d}\right)^{-1} Z_d^{\mathrm{EJ}_c}\right]^{-1} \quad (26)$$

$$Z_{\rm mul}^B = Z_c^{\mathrm{EM}_d} - Z_c^{\mathrm{EJ}_d}\left(Z_d^{\mathrm{EJ}_d}\right)^{-1} Z_d^{\mathrm{EM}_d}. \quad (27)$$

By considering (20) and (21), we have

$$J_{\rm cn} = -Z_{\rm mul}^A Z_{\rm mul}^B M_{\rm dn} \quad (28)$$

$$J_{\rm dn} = \left[-\left(Z_d^{\mathrm{EJ}_d}\right)^{-1} Z_d^{\mathrm{EM}_d} + \left(Z_d^{\mathrm{EJ}_d}\right)^{-1} Z_d^{\mathrm{EJ}_c} Z_{\rm mul}^A Z_{\rm mul}^B\right] M_{\rm dn}. \quad (29)$$

Substituting (28) and (29) into (22), we have

$$\begin{aligned} &Z_d^{\mathrm{HJ}_c} J_{\rm cn} + Z_d^{\mathrm{HJ}_d} J_{\rm dn} + Z_d^{\mathrm{HM}_d} M_{\rm dn} \\ &= \begin{bmatrix} Z_d^{\mathrm{HM}_d} - Z_d^{\mathrm{HJ}_d}\left(Z_d^{\mathrm{EJ}_d}\right)^{-1} Z_d^{\mathrm{EM}_d} \\ -Z_d^{\mathrm{HJ}_c} Z_{\rm mul}^A Z_{\rm mul}^B + Z_d^{\mathrm{HJ}_d}\left(Z_d^{\mathrm{EJ}_d}\right)^{-1} Z_d^{\mathrm{EJ}_c} Z_{\rm mul}^A Z_{\rm mul}^B \end{bmatrix} M_{\rm dn} \\ &= Z^M M_{\rm dn}. \end{aligned} \quad (30)$$

The submatrices $Z_c^{\mathrm{EJ}_c}$, $Z_d^{\mathrm{EJ}_d}$, $Z_d^{\mathrm{EM}_d}$, $Z_d^{\mathrm{HJ}_d}$, and $Z_d^{\mathrm{HM}_d}$ are symmetric. Because $Z_d^{\mathrm{EM}_d} = -Z_d^{\mathrm{HJ}_d}$, $Z_d^{\mathrm{EJ}_c} = (Z_c^{\mathrm{EJ}_d})^T$, and $Z_d^{\mathrm{HJ}_c} = (Z_c^{\mathrm{EM}_d})^T$, one can get $Z^M = (Z^M)^T$, where the superscript "T" denotes the transpose of the matrix in the brackets. Therefore, Z^M is also a symmetric matrix. It can be expressed in terms of its Hermitian parts as $Z^M = R^M + jX^M$ where

$$R^M = \frac{Z^M + (Z^M)^*}{2} \quad (31)$$

$$X^M = \frac{Z^M - (Z^M)^*}{2j} \quad (32)$$

where the asterisk denotes the complex conjugation.

As there is no actual impressed source inside region V_1, the net complex power is zero. Following Poynting's theorem in source-free region, we have:

$$\begin{aligned} P^{(1)} = &\oint_{S_d + S_\infty} \mathbf{E}_n^{(1)} \times \left(\mathbf{H}_n^{(1)}\right)^* \mathbf{dS} \\ &+ j\omega \int_{V_1} \left(\mu_1 \left|\mathbf{H}_n^{(1)}\right|^2 - \varepsilon_1 \left|\mathbf{E}_n^{(1)}\right|^2\right) dV = 0 \end{aligned} \quad (33)$$

where S_∞ denotes the infinite radiation sphere, as shown in Fig. 1. The surface integration gives the complex power exiting out of the region, and the volume integration multiplied by $j\omega$ gives the imaginary power stored in region V_1. Considering the definition of the outward normal unit vector on surfaces S_d and S_∞ (as shown in Fig. 1), (33) reduces to

$$\begin{aligned} P^{(1)} = &-\oint_{S_d} \mathbf{E}_n^{(1)} \times \left(\mathbf{H}_n^{(1)}\right)^* \cdot \hat{n} dS + \oint_{S_\infty} \mathbf{E}_n^{(1)} \times \left(\mathbf{H}_n^{(1)}\right)^* \cdot \hat{n} dS \\ &+ j\omega \int_{V_1} \left(\mu_1 \left|\mathbf{H}_n^{(1)}\right|^2 - \varepsilon_1 \left|\mathbf{E}_n^{(1)}\right|^2\right) dV = 0. \end{aligned} \quad (34)$$

Therefore

$$\begin{aligned} &\oint_{S_d} \mathbf{E}_n^{(1)} \times \left(\mathbf{H}_n^{(1)}\right)^* \cdot \hat{n} dS \\ &\quad = \oint_{S_\infty} \mathbf{E}_n^{(1)} \times \left(\mathbf{H}_n^{(1)}\right)^* \cdot \hat{n} dS \\ &\qquad + j\omega \int_{V_1} \left(\mu_1 \left|\mathbf{H}_n^{(1)}\right|^2 - \varepsilon_1 \left|\mathbf{E}_n^{(1)}\right|^2\right) dV. \end{aligned} \quad (35)$$

Similarly, there is also no actual impressed source inside region V_2. Following Poynting's theorem in region V_2, we have:

$$P^{(2)} = \oint_{S_d+S_c} \mathbf{E}_n^{(2)} \times \left(\mathbf{H}_n^{(2)}\right)^* \mathbf{dS} + j\omega \int_{V_2} \left(\mu_2 \left|\mathbf{H}_n^{(2)}\right|^2 - \varepsilon_2 \left|\mathbf{E}_n^{(2)}\right|^2\right) dV = 0. \quad (36)$$

Again, when the definition of the outward normal unit vector is considered, we have

$$\oint_{S_c} \mathbf{E}_n^{(2)} \times \left(\mathbf{H}_n^{(2)}\right)^* \cdot \hat{n} dS - \oint_{S_d} \mathbf{E}_n^{(2)} \times \left(\mathbf{H}_n^{(2)}\right)^* \cdot \hat{n} dS = j\omega \int_{V_2} \left(\mu_2 \left|\mathbf{H}_n^{(2)}\right|^2 - \varepsilon_2 \left|\mathbf{E}_n^{(2)}\right|^2\right) dV. \quad (37)$$

Based on (37), and considering $\mathbf{E}_n^{(2)} \times \mathbf{H}_n^{(2)} \cdot \hat{n} = \hat{n} \times \mathbf{E}_n^{(2)} \cdot \mathbf{H}_n^{(2)} = 0$ on S_c, we obtain

$$-\oint_{S_d} \mathbf{E}_n^{(2)} \times \left(\mathbf{H}_n^{(2)}\right)^* \cdot \hat{n} dS = j\omega \int_{V_2} \left(\mu_2 \left|\mathbf{H}_n^{(2)}\right|^2 - \varepsilon_2 \left|\mathbf{E}_n^{(2)}\right|^2\right) dV. \quad (38)$$

Adding (35) and (38) yields

$$\oint_{S_d} \mathbf{E}_n^{(1)} \times \left(\mathbf{H}_n^{(1)}\right)^* \cdot \hat{n} dS - \oint_{S_d} \mathbf{E}_n^{(2)} \times \left(\mathbf{H}_n^{(2)}\right)^* \cdot \hat{n} dS = \oint_{S_\infty} \mathbf{E}_n^{(1)} \times \left(\mathbf{H}_n^{(1)}\right)^* \cdot \hat{n} dS + j\omega \int_{V_1} \left(\mu_1 \left|\mathbf{H}_n^{(1)}\right|^2 - \varepsilon_1 \left|\mathbf{E}_n^{(1)}\right|^2\right) dV + j\omega \int_{V_2} \left(\mu_2 \left|\mathbf{H}_n^{(2)}\right|^2 - \varepsilon_2 \left|\mathbf{E}_n^{(2)}\right|^2\right) dV. \quad (39)$$

Using (22), (25), and (30), the field tangential continuity in (21), and invoking vector identity $(\mathbf{a} \times \mathbf{b}) \cdot \mathbf{c} = (\mathbf{c} \times \mathbf{a}) \cdot \mathbf{b}$, we obtain

$$\begin{aligned}
&\oint_{S_d} \mathbf{E}_n^{(1)} \times \left(\mathbf{H}_n^{(1)}\right)^* \cdot \hat{n} dS - \oint_{S_d} \mathbf{E}_n^{(2)} \times \left(\mathbf{H}_n^{(2)}\right)^* \cdot \hat{n} dS \\
&= \oint_{S_d} \left(\mathbf{H}_n^{(1)}\right)^* \cdot \left(\hat{n} \times \mathbf{E}_n^{(1)}\right) dS - \oint_{S_d} \left(\mathbf{H}_n^{(2)}\right)^* \cdot \left(\hat{n} \times \mathbf{E}_n^{(2)}\right) dS \\
&= \oint_{S_d} \left[\left(\mathbf{H}_n^{(1)}\right)^* - \left(\mathbf{H}_n^{(2)}\right)^*\right] \cdot \left(\hat{n} \times \mathbf{E}_n^{(1)}\right) dS \\
&= -\oint_{S_d} \left[\left(\mathbf{H}_n^{(1)}\right)^* - \left(\mathbf{H}_n^{(2)}\right)^*\right]_{\tan} \cdot \mathbf{M}_{\mathrm{dn}} dS \\
&= -\oint_{S_d} \left[\left(\mathbf{H}_n^{(1)}\right)^* - \left(\mathbf{H}_n^{(2)}\right)^*\right]_{\tan} \cdot \sum_{k=1}^{N_d} M_{\mathrm{dn},k} \mathbf{f}_k dS \\
&= \sum_{k=1}^{N_d} M_{\mathrm{dn},k} \left(-\oint_{S_d} \mathbf{f}_k \cdot \left[\left(\mathbf{H}_n^{(1)}\right)^* - \left(\mathbf{H}_n^{(2)}\right)^*\right]_{\tan} dS\right) \\
&= \langle (Z^M M_{\mathrm{dn}})^*, M_{\mathrm{dn}} \rangle
\end{aligned} \quad (40)$$

where $M_{\mathrm{dn},k}$ is the kth element in the vector of magnetic current coefficient, and the inner product is defined for the Hilbert space on the equivalent surface S_d. Applying (39) and $Z^M = R^M + jX^M$ to (40), we have

$$\begin{aligned}
P^{\mathrm{total}} &= \langle (M_{\mathrm{dn}})^*, Z^M M_{\mathrm{dn}} \rangle \\
&= \langle (M_{\mathrm{dn}})^*, (R^M + jX^M) M_{\mathrm{dn}} \rangle \\
&= \langle (M_{\mathrm{dn}})^*, R^M M_{\mathrm{dn}} \rangle + j \langle (M_{\mathrm{dn}})^*, X^M M_{\mathrm{dn}} \rangle \\
&= \langle (Z^M M_{\mathrm{dn}})^*, M_{\mathrm{dn}} \rangle^* \\
&= \left[\oint_{S_\infty} \mathbf{E}_n^{(1)} \times \left(\mathbf{H}_n^{(1)}\right)^* \cdot \hat{n} dS\right]^* \\
&\quad + \left[\begin{array}{l} j\omega \displaystyle\int_{V_1} \left(\mu_1 \left|\mathbf{H}_n^{(1)}\right|^2 - \varepsilon_1 \left|\mathbf{E}_n^{(1)}\right|^2\right) dV \\ + j\omega \displaystyle\int_{V_2} \left(\mu_2 \left|\mathbf{H}_n^{(2)}\right|^2 - \varepsilon_2 \left|\mathbf{E}_n^{(2)}\right|^2\right) dV \end{array}\right]^*.
\end{aligned} \quad (41)$$

And we further obtain

$$\begin{aligned}
&\langle (M_{\mathrm{dn}})^*, R^M M_{\mathrm{dn}} \rangle + j \langle (M_{\mathrm{dn}})^*, X^M M_{\mathrm{dn}} \rangle \\
&\quad = \oint_{S_\infty} \mathbf{E}_n^{(1)} \times \left(\mathbf{H}_n^{(1)}\right)^* \cdot \hat{n} dS \\
&\qquad + \left[\begin{array}{l} j\omega \displaystyle\int_{V_1} \left(\varepsilon_1 \left|\mathbf{E}_n^{(1)}\right|^2 - \mu_1 \left|\mathbf{H}_n^{(1)}\right|^2\right) dV \\ + j\omega \displaystyle\int_{V_2} \left(\varepsilon_2 \left|\mathbf{E}_n^{(2)}\right|^2 - \mu_2 \left|\mathbf{H}_n^{(2)}\right|^2\right) dV \end{array}\right].
\end{aligned} \quad (42)$$

In (42), the first surface integration over the infinite sphere represents the real power radiated into the free space. The two volume integrations represent the imaginary power stored in region V_1 and V_2, respectively. Moreover, we also observe from (42) that $\langle (M_{\mathrm{dn}})^*, R^M M_{\mathrm{dn}} \rangle$ and $\langle (M_{\mathrm{dn}})^*, X^M M_{\mathrm{dn}} \rangle$ represent the radiation power and stored energy, respectively. Therefore, $\langle (M_{\mathrm{dn}})^*, R^M M_{\mathrm{dn}} \rangle$ must be nonnegative as the radiated power must be greater or equal to zero. It indicates R^M is a semipositive definite matrix.

In radiation system designs, we aim to improve the radiation efficiency by enhancing the radiation power and reducing the stored energy for a given external feeding power. It can be mathematically represented as the minimization of the following function:

$$f(M_{\mathrm{dn}}) = \frac{P_{\mathrm{store}}}{P_{\mathrm{radiation}}} = \frac{\langle (M_{\mathrm{dn}})^*, X^M M_{\mathrm{dn}} \rangle}{\langle (M_{\mathrm{dn}})^*, R^M M_{\mathrm{dn}} \rangle}. \quad (43)$$

A variational expression in terms of M_{dn} results in the following generalized eigenvalue equation:

$$X^M M_{\mathrm{dn}} = \lambda_n R^M M_{\mathrm{dn}}. \quad (44)$$

As both R^M and X^M are symmetric matrices, the eigenvalues and characteristic currents are real. Therefore

$$\begin{aligned}
\langle (M_{\mathrm{dn}})^*, (R^M + jX^M) M_{\mathrm{dn}} \rangle &= \langle M_{\mathrm{dn}}, (R^M + jX^M) M_{\mathrm{dn}} \rangle \\
&= (1 + j\lambda_n) \langle M_{\mathrm{dn}}, R^M M_{\mathrm{dn}} \rangle.
\end{aligned} \quad (45)$$

Each characteristic current M_{dn} can be normalized, such that it radiates unit power

$$\langle M_{\mathrm{dn}}, R^M M_{\mathrm{dn}} \rangle = 1. \quad (46)$$

After normalization, the orthogonality relationship among characteristic currents M_{dn} is given by

$$\langle M_{\mathrm{dm}}, Z^M M_{\mathrm{dn}} \rangle = (1 + j\lambda_n) \delta_{\mathrm{mn}} \quad (47)$$

where δ_{mn} is the Kronecker delta function ($\delta_{\mathrm{mn}} = 1$ for $m = n$ and $\delta_{\mathrm{mn}} = 0$ for $m \neq n$).

In addition, considering the normalized characteristic currents M_{dn}, we can obtain (48) from (42) and (47)

$$\begin{aligned}\oint_{S_\infty} \mathbf{E}_m^{(1)} \times \left(\mathbf{H}_n^{(1)}\right)^* \cdot \hat{n} dS &+ j\omega \int_{V_1} \left[\mu_1 \mathbf{H}_m^{(1)} \cdot \left(\mathbf{H}_n^{(1)}\right)^* - \varepsilon_1 \mathbf{E}_m^{(1)} \cdot \left(\mathbf{E}_n^{(1)}\right)^*\right] dV \\ &+ j\omega \int_{V_2} \left[\mu_2 \mathbf{H}_m^{(2)} \cdot \left(\mathbf{H}_n^{(2)}\right)^* - \varepsilon_2 \mathbf{E}_m^{(2)} \cdot \left(\mathbf{E}_n^{(2)}\right)^*\right] dV \\ &= (1 - j\lambda_n)\delta_{\mathrm{mn}}. \end{aligned} \tag{48}$$

As the characteristic fields are outward traveling waves on the infinite radiation sphere S_∞, they satisfy

$$\mathbf{E}_n^{(1)} = \eta_1 \mathbf{H}_n^{(1)} \times \hat{n}. \tag{49}$$

Considering the relationship between electric and magnetic fields in (49), by interchanging m and n, and taking the complex conjugate of (48), and adding it to (48) itself yields

$$\frac{1}{\eta_1} \oint_{S_\infty} \mathbf{E}_m^{(1)} \cdot \left(\mathbf{E}_n^{(1)}\right)^* dS = \delta_{\mathrm{mn}}. \tag{50}$$

It is evident that characteristic fields form an orthogonal set in the far-field region.

It is important to point out that the physical interpretations of the eigenvalues solved from (44) are different from those defined in CM theory for PEC bodies [2]. As can be observed from (42)–(45), the eigenvalues solved from (44) possess the following physical meanings.

1) $\lambda_n = 0$ indicates the mode is in resonance.
2) $\lambda_n < 0$ indicates the system stores more magnetic energy than electric energy.
3) $\lambda_n > 0$ indicates the system stores more electric energy than magnetic energy.

Evidently, signs of the eigenvalues solved from (44) have contrary meanings as those in CM theory of PEC bodies [2]. In the case the radiation power is normalized, the eigenvalues represent the amount of reactive energy in the system.

D. Magnetic Field Continuity

Let the right-hand side of (22) equals to zero, and it ensures the magnetic fields tangential continuity across the interface between regions V_1 and V_2. Again, let us first define two new matrices

$$Z_{\mathrm{mul}}^A = \left[Z_c^{\mathrm{EJ}_c} - Z_c^{\mathrm{EM}_d} \left(Z_d^{\mathrm{HM}_d}\right)^{-1} Z_d^{\mathrm{HJ}_c}\right]^{-1} \tag{51}$$

$$Z_{\mathrm{mul}}^B = Z_c^{\mathrm{EJ}_d} - Z_c^{\mathrm{EM}_d} \left(Z_d^{\mathrm{HM}_d}\right)^{-1} Z_d^{\mathrm{HJ}_d}. \tag{52}$$

Considering (20) and (22), we have

$$\begin{aligned} &Z_d^{\mathrm{EJ}_c} J_{\mathrm{cn}} + Z_d^{\mathrm{EJ}_d} J_{\mathrm{dn}} + Z_d^{\mathrm{EM}_d} M_{\mathrm{dn}} \\ &= \begin{bmatrix} Z_d^{\mathrm{EJ}_d} - Z_d^{\mathrm{EM}_d} \left(Z_d^{\mathrm{HM}_d}\right)^{-1} Z_d^{\mathrm{HJ}_d} \\ -Z_d^{\mathrm{EJ}_c} Z_{\mathrm{mul}}^A Z_{\mathrm{mul}}^B + Z_d^{\mathrm{EM}_d} \left(Z_d^{\mathrm{HM}_d}\right)^{-1} Z_d^{\mathrm{HJ}_c} Z_{\mathrm{mul}}^A Z_{\mathrm{mul}}^B \end{bmatrix} J_{\mathrm{dn}} \\ &= Z^E J_{\mathrm{dn}}. \end{aligned} \tag{53}$$

It is easy to observe that $Z^E = (Z^E)^T$. Therefore, Z^E is a symmetric matrix and can be expressed in terms of its Hermitian parts as $Z^E = R^E + jX^E$, where

$$R^E = \frac{Z^E + (Z^E)^*}{2} \tag{54}$$

$$X^E = \frac{Z^E - (Z^E)^*}{2j}. \tag{55}$$

Following the similar procedure in Section II-C, we can obtain:

$$\begin{aligned} P^{\mathrm{total}} &= \langle (J_{\mathrm{dn}})^*, Z^E J_{\mathrm{dn}} \rangle \\ &= \langle (J_{\mathrm{dn}})^*, (R^E + jX^E) J_{\mathrm{dn}} \rangle \\ &= \langle (J_{\mathrm{dn}})^*, R^E J_{\mathrm{dn}} \rangle + j \langle (J_{\mathrm{dn}})^*, X^E J_{\mathrm{dn}} \rangle \\ &= \oint_{S_\infty} \mathbf{E}_n^{(1)} \times \left(\mathbf{H}_n^{(1)}\right)^* \cdot \hat{n} dS \\ &\quad + j\omega \int_{V_1} \left(\mu_1 \left|\mathbf{H}_n^{(1)}\right|^2 - \varepsilon_1 \left|\mathbf{E}_n^{(1)}\right|^2\right) dV \\ &\quad + j\omega \int_{V_2} \left(\mu_2 \left|\mathbf{H}_n^{(2)}\right|^2 - \varepsilon_2 \left|\mathbf{E}_n^{(2)}\right|^2\right) dV. \end{aligned} \tag{56}$$

Similar to the discussions in Section II-C, the first surface integration on the infinite sphere represents the radiation power into the free space. The last two volume integrations represent the stored energy in region V_1 and V_2, respectively. Furthermore, it can be further found that $\langle (J_{\mathrm{dn}})^*, R^E J_{\mathrm{dn}} \rangle$ and $\langle (J_{\mathrm{dn}})^*, X^E J_{\mathrm{dn}} \rangle$ represent the radiation power and stored energy, respectively. We can also find that R^E is a semipositive definite matrix.

Similarly, a variational expression in terms of J_{dn} gives the following generalized eigenvalue equation:

$$X^E J_{\mathrm{dn}} = \lambda_n R^E J_{\mathrm{dn}}. \tag{57}$$

Obviously, the resultant eigenvalues and characteristic currents solved from (57) are real. The eigenvalues have exactly the same physical interpretations as those in CM theory of PEC bodies. Moreover, the characteristic currents can be normalized to offer unit radiation power and we can also get the orthogonality of the characteristic fields in far-field region.

In summary, the two types of generalized eigenvalue equations both give the same resonant frequencies and characteristic fields for the same dielectric coated conducting bodies. Numerical results are presented in Section III to illustrate the effectiveness of the proposed CM formulations.

III. Numerical Results and Discussion

To confirm the validity of the proposed CM theory, examples, including dielectric coated conducting cuboid and dielectric coated conducting warhead, are first considered. Because there are little available modal analysis results in the literature for validations, comparison studies between fictitious air coated conducting bodies and isolated conducting bodies are carried out first. Conducting bodies with true dielectric coatings are followed. Then, a more practical example is presented to illustrate the effectiveness in the modal analysis of a hemispherical dielectric-resonator antenna (DRA) with a concentric conductor. Good agreement is observed in the comparison between the CM analysis results and those obtained in other approaches and experiments.

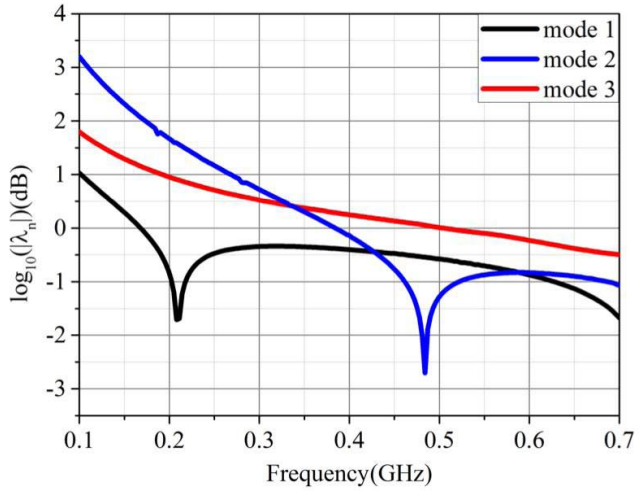

Fig. 2. Eigenvalues of the isolated conducting cuboid.

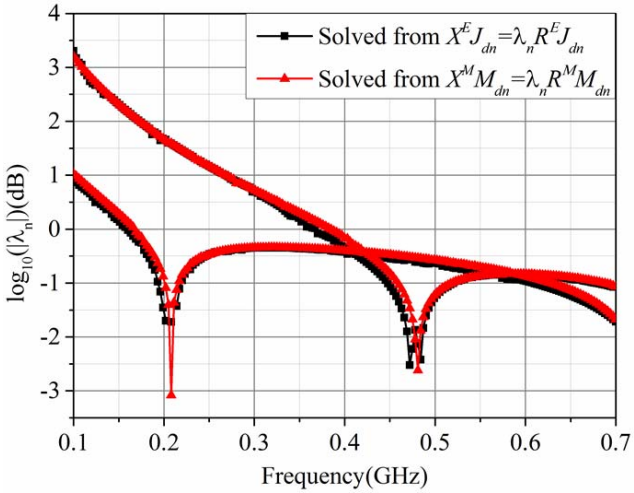

Fig. 4. Eigenvalues of the fictitious air coated conducting cuboid with a coatings thickness of 0.2 h.

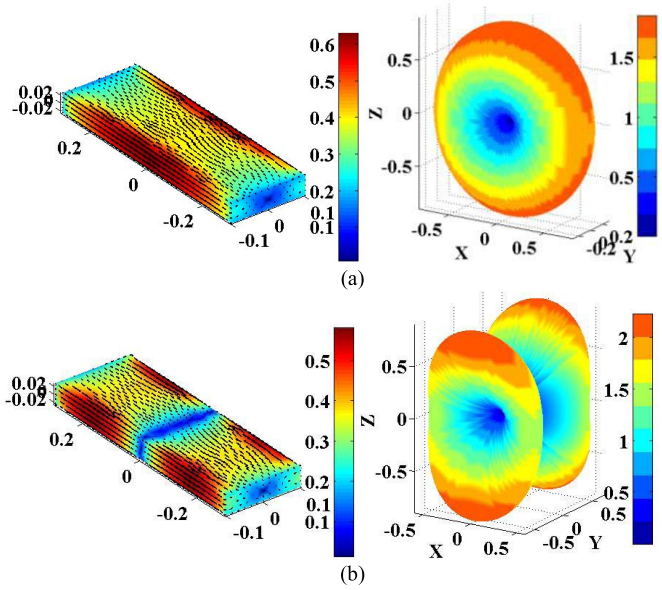

Fig. 3. Characteristic currents (left) and characteristic fields (right) of resonant modes of the isolated conducting cuboid at their own resonant frequencies. (a) Mode 1 resonates at 0.208 GHz. (b) Mode 2 resonates at 0.484 GHz.

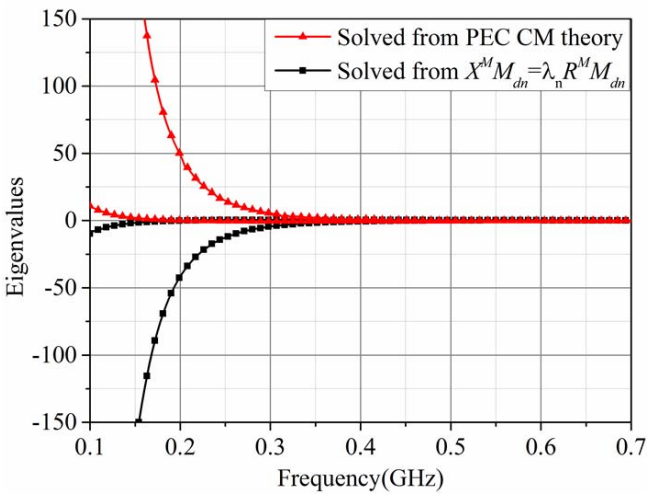

Fig. 5. Comparison of eigenvalues solved from $X^M M_{\mathrm{dn}} = \lambda_n R^M M_{\mathrm{dn}}$ for the fictitious air coated conducting cuboid and PEC CM theory for the isolated conducting cuboid.

A. Dielectric Coated Conducting Cuboid

A fictitious air coated conducting cuboid with the sizes of $h \times l \times w = 0.05 \times 0.6 \times 0.2$ m^3 is first studied. We assume the thickness of the air coatings is 0.2 h. Example with true dielectric coatings ($\varepsilon_r = 6.0$) is then studied and discussed to show the effect of the dielectric coatings on resonant frequencies. Owing to the well-developed CM theory for PEC bodies, we directly apply the CM formulation based on the EFIE [2] throughout this paper without additional explanations.

In Fig. 2, the absolute values of the eigenvalues in log scale are presented. The valleys of the curves clearly show the resonant frequencies over the interested frequency band. As can be seen, there are two dominant modes within the frequency band of 0.1–0.7 GHz. The two modes resonate at 0.208 and 0.484 GHz, respectively. Fig. 3 shows the characteristic currents and characteristic fields of the two modes at their own resonant frequencies. It helps us to better understand the modal behavior of the two modes.

Modal analysis for the same conducting cuboid with fictitious air coatings is then performed with the proposed generalized eigenvalue equations. Fig. 4 shows eigenvalues of the conducting cuboid with the fictitious air coatings of thickness 0.2 h. As can be seen, the two types of generalized eigenvalue equations show reasonable agreement and characterize the same resonant characteristics. In addition, in the air coating case, the eigenvalues also agree well with those in Fig. 2. This example well illustrates that the proposed CM formulation is able to predict the resonant frequencies accurately.

Fig. 5 compares the pure eigenvalues obtained from the proposed CM formulation and the CM formulation for PEC bodies, respectively. As can be observed, the eigenvalues solved from the two approaches have the same magnitude but opposite signs. It is easy to understand this difference from (42) and the physical meanings of the eigenvalues in (44).

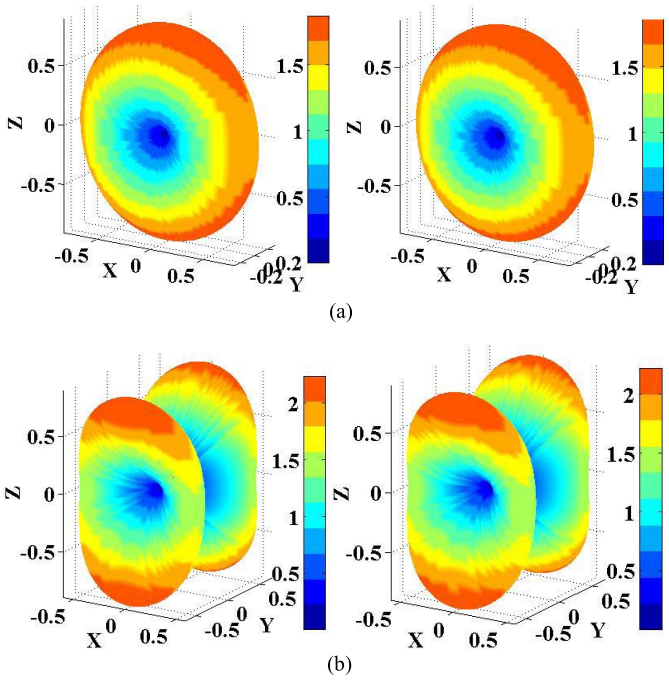

Fig. 6. Characteristic fields of the resonant modes of the fictitious air coated conducting cuboid at their own resonant frequencies. The coatings thickness is 0.2 h. The fields are computed from $X^E J_{\rm dn} = \lambda_n R^E J_{\rm dn}$ (left) and $X^M M_{\rm dn} = \lambda_n R^M M_{\rm dn}$ (right), respectively. (a) Mode 1. (b) Mode 2.

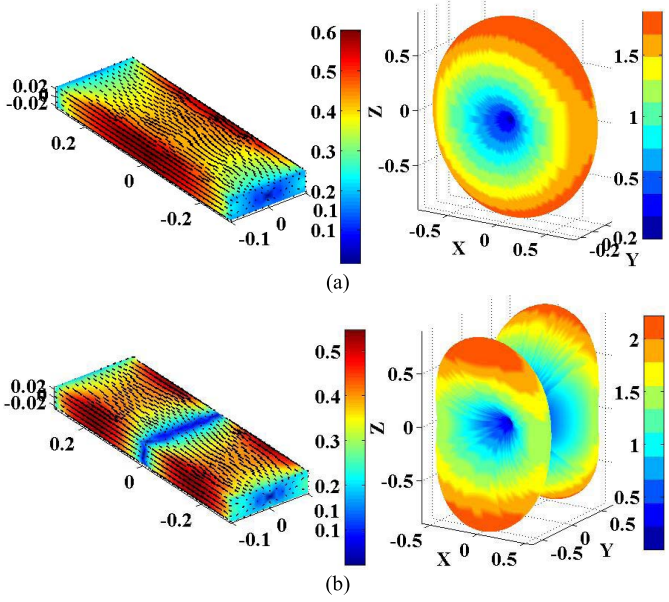

Fig. 7. Characteristic currents (left) and characteristic fields (right) of the resonant modes of the fictitious air coated conducting cuboid at their own resonant frequencies. The coatings thickness is 0.2 h. The fields are computed from $X^M M_{\rm dn} = \lambda_n R^M M_{\rm dn}$. (a) Mode 1 resonates at 0.208 GHz. (b) Mode 2 resonates at 0.481 GHz.

The characteristic fields solved from $X^E J_{\rm dn} = \lambda_n R^E J_{\rm dn}$ and $X^M M_{\rm dn} = \lambda_n R^M M_{\rm dn}$ are compared in Fig. 6. As can be seen, good agreement is observed. The characteristic currents and characteristic fields of the dominant modes solved from $X^M M_{\rm dn} = \lambda_n R^M M_{\rm dn}$ at their own resonant frequencies are shown in Fig. 7. As compared with the isolated case, as shown in Fig. 3, the agreement is pretty good. In summary, the comparison study for the characteristic fields well illustrates

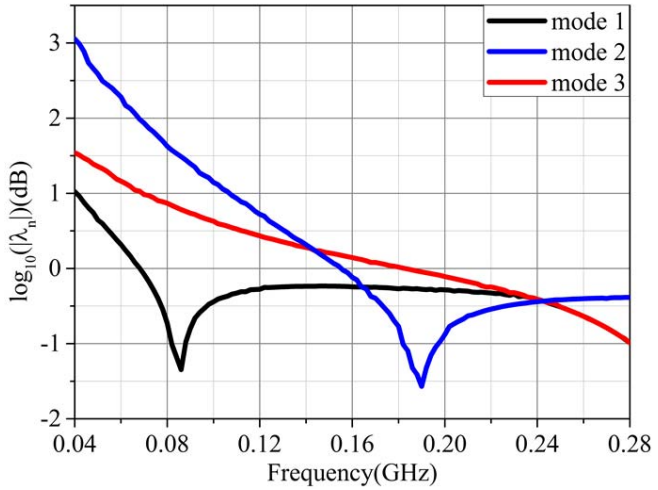

Fig. 8. Eigenvalues of dielectric coated conducting cuboid computed from $X^M M_{\rm dn} = \lambda_n R^M M_{\rm dn}$. The dielectric coating material is of $\varepsilon_r = 6.0$ and the dielectric coating thickness is 0.2 h.

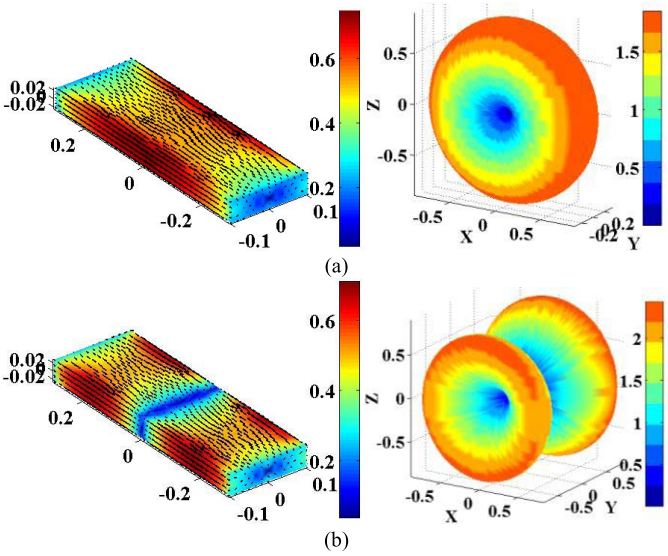

Fig. 9. Characteristic currents (left) and characteristic fields (right) of the resonant modes of the dielectric coated conducting cuboid at their own resonant frequencies. The coatings thickness is 0.2 h. The fields are computed from $X^M M_{\rm dn} = \lambda_n R^M M_{\rm dn}$. (a) Mode 1 resonates at 0.084 GHz. (b) Mode 2 resonates at 0.19 GHz.

the effectiveness of the proposed CM formulation in solving the modal fields in both near and far fields regions.

Then modal analysis for dielectric coated conducting cuboid is then performed. The dielectric coatings thickness is 0.2 h and the relative dielectric permittivity is $\varepsilon_r = 6.0$. The eigenvalues for the dielectric coated conducting cuboid are presented in Fig. 8. As compared with the isolated or air-coated cases, mode 1 and mode 2 resonate at lower frequencies. The classic EM theory states that dielectric coatings will increase the electrical sizes. In the other word, it will lower the resonant frequencies. Thus, the observation from Fig. 8 well shows the true physics happened when dielectric material is loaded.

To further show the impact of the dielectric coatings, Fig. 9 shows the characteristic currents and characteristic fields of the two resonant modes at their resonant frequencies. As compared with the isolated or air-coated cases, the modal fields suffer

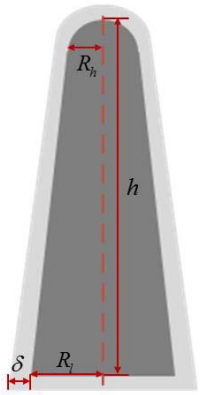

Fig. 10. Geometry of the dielectric coated conducting warhead: $R_l = 10$ mm, $R_h = 5$ mm, $h = 65$ mm, and $\delta = 1$ mm (the light gray represents the dielectric coatings and the dark gray denotes the conducting warhead).

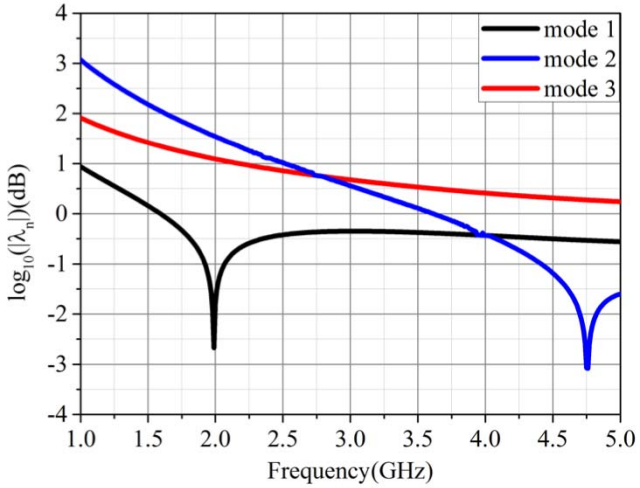

Fig. 11. Eigenvalues of the isolated conducting warhead.

little variations in mode 1 and a little bit large variations in mode 2. However, the modal field property roughly follows those of the noncoated case.

B. Simplified Dielectric Coated Conducting Warhead

As the second example, the CM analysis of a simplified dielectric coated conducting warhead is presented. The geometry and dimensions are given in Fig. 10. Following the same procedure, the fictitious air coated and true dielectric coated conducting warheads are studied, respectively.

In Fig. 11, the absolute values of the eigenvalues in log scale for the isolated conducting warhead solved from the EFIE-based CM theory are presented. The resultant curves clearly show the resonant frequencies of the dominant modes. It can be observed that the first two modes of the isolated conducting warhead resonate at 2.0 and 4.76 GHz in the frequency range of 1.0–5.0 GHz. The characteristic currents and characteristic fields of the resonant modes at their own resonant frequencies are shown in Fig. 12.

Then, the CM analysis for the fictitious air coated conducting warhead is carried out by using $X^M M_{\rm dn} = \lambda_n R^M M_{\rm dn}$. As can be observed from the eigenvalues shown in Fig. 13, mode 1 and mode 2 resonate at 1.99 and 4.81 GHz,

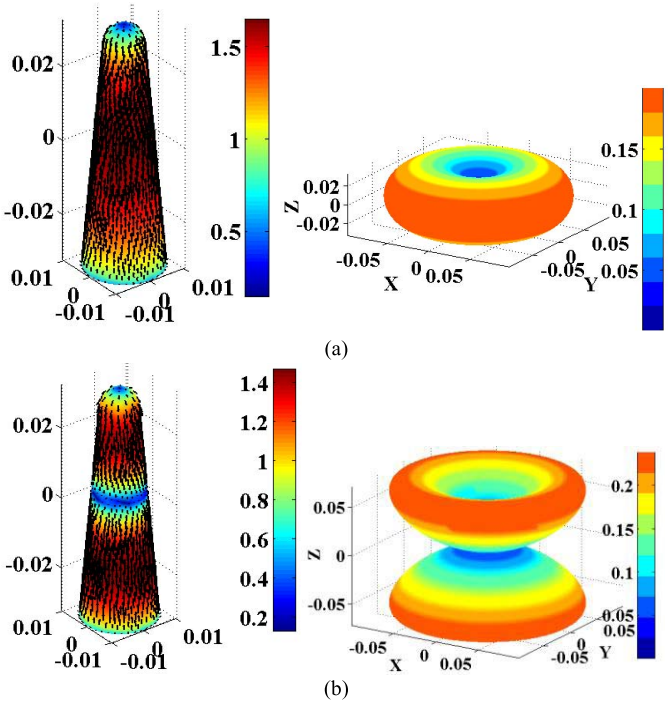

Fig. 12. Characteristic currents (left) and characteristic fields (right) of the resonant modes of the isolated conducting warhead at their own resonant frequencies. (a) Mode 1 resonates at 2.0 GHz. (b) Mode 2 resonates at 4.76 GHz.

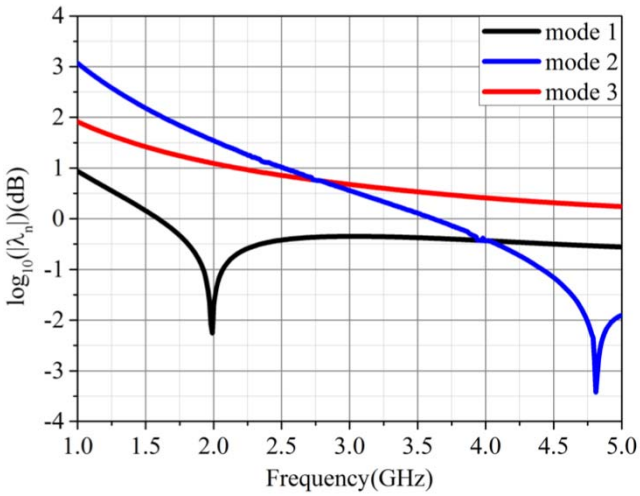

Fig. 13. Eigenvalues of the fictitious air coated conducting warhead computed from $X^M M_{\rm dn} = \lambda_n R^M M_{\rm dn}$.

respectively. As compared with the isolated case in Fig. 11, the relative error is less than 1%. It again well demonstrates the accuracy of the proposed CM formulations in the prediction of resonant frequencies.

The characteristic currents and characteristic fields of the resonant modes at their own resonant frequencies are shown in Fig. 14. As compared with those in Fig. 12, the resultant characteristic currents and characteristic fields achieve good agreement. It again validates the accuracy of the proposed CM formulations in solving of modal fields.

Finally, a conducting warhead coated by dielectric material with a relative permittivity of 6 and a thickness of 1 mm is investigated. The calculated eigenvalues from the

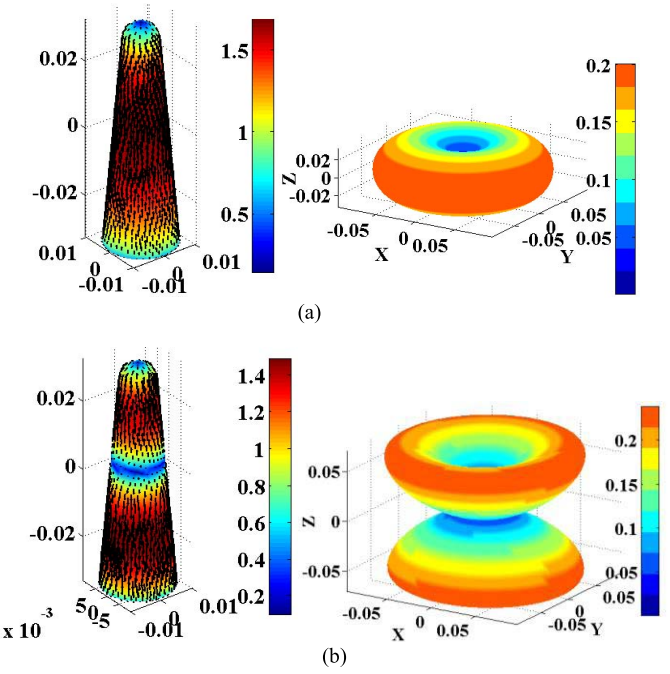

Fig. 14. Characteristic currents (left) and characteristic fields (right) of the fictitious air coated conducting warhead at resonant frequencies. The fields are solved from $X^M M_{\rm dn} = \lambda_n R^M M_{\rm dn}$. (a) Mode 1 resonates at 2.0 GHz. (b) Mode 2 resonates at 4.81 GHz.

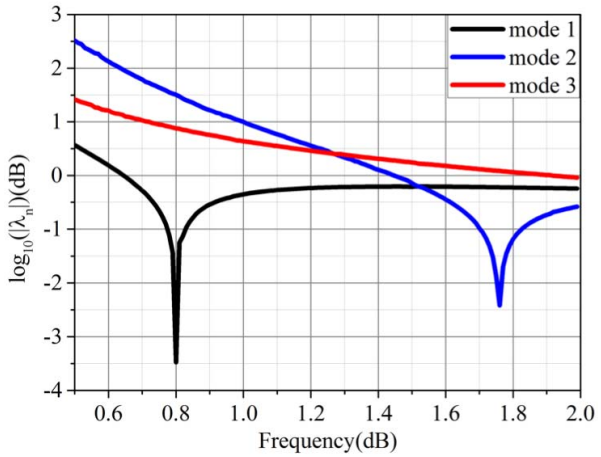

Fig. 15. Eigenvalues of the dielectric coated conducting warhead computed from $X^M M_{\rm dn} = \lambda_n R^M M_{\rm dn}$.

generalized eigenvalue equation $X^M M_{\rm dn} = \lambda_n R^M M_{\rm dn}$ are given in Fig. 15. As can be seen, the resonant frequencies of the first two modes also shift toward lower frequencies. Mode 1 and mode 2 resonate at 0.8 and 1.76 GHz, respectively. The characteristic currents and characteristic fields of the dielectric coated warhead are presented in Fig. 16. As compared with modal fields for the isolated and air-coated cases, they also suffer from little variations due to the dielectric loadings.

The coatings for the conducting cuboid and warhead have the same property. It indicates the dielectric coatings introduce the same amount of resonant frequency shifting in the two examples. Table I compares the resonant frequency shifting in the two examples. This phenomenon provides valuable information on how to adjust the resonant characteristics of conducting bodies through using dielectric coatings.

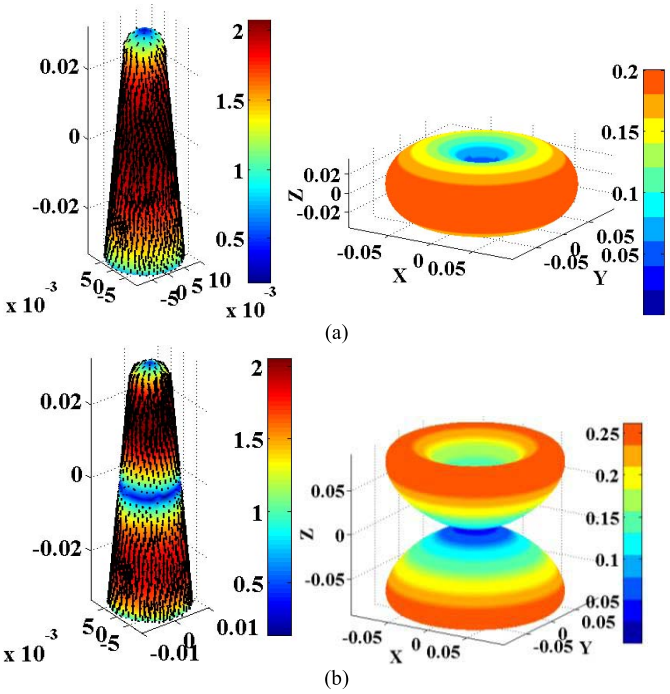

Fig. 16. Characteristic currents (left) and characteristic fields (right) of the resonant modes of the dielectric coated conducting warhead at their own resonant frequencies. The fields are solved from $X^M M_{\rm dn} = \lambda_n R^M M_{\rm dn}$. (a) Mode 1 resonates at 0.8 GHz. (b) Mode 2 resonates at 1.76 GHz.

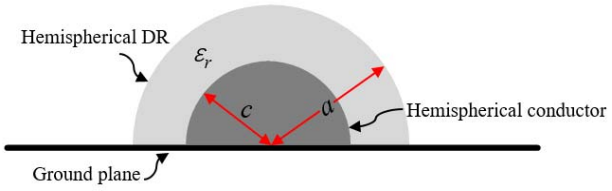

Fig. 17. Configuration of the hemispherical DRA with a concentric conductor: $a = 12.5$ mm and $c = 8$ mm.

TABLE I
COMPARISON OF RESONANT FREQUENCY SHIFTING IN TWO CASES

Model Details	Coated Metal Cuboid		Coated Metal Warhead	
	Mode 1	Mode 2	Mode 1	Mode 2
f_{air} for air coatings(GHz)	0.208	0.484	2.0	4.81
f_{die} for dielectric coatings (GHz)	0.084	0.19	0.8	1.76
Frequency ratio (f_{air}/f_{die})	2.48	2.55	2.50	2.73

f_{air} and f_{die} mean resonant frequencies.

C. CM Analysis for Practical Antennas

To further demonstrate the accuracy of the proposed CM theory, the resonant frequencies of a hemispherical DRA with a concentric conductor are investigated [28]. The antenna geometry and dimensions are shown in Fig. 17. It can be regarded as a dielectric coated conducting sphere when the image theory is applied for removing the ground plane. The proposed CM theory is thus suitable to solve its resonant frequencies.

In [28], the resonant frequency for the TE_{111} mode of a DRA is determined by analytical formulations obtained using

TABLE II
COMPARISON OF RESONANT FREQUENCIES FROM THE TWO METHODS

	The outer radius and inner radius of the DRA are fixed at a = 12.5 mm and c = 8 mm		
	ε_r=10	ε_r=20	ε_r=40
f_r from [28] (GHz)	5.826	4.218	3.043
f_r from the proposed theory (GHz)	5.80	4.16	2.99
Relative error (%)	0.4	1.4	1.7

f_r means resonant frequency for TE mode.

the curve fitting technique. For convenience purpose, they are quoted as follows:

$$f_r = A_1(\sqrt{\varepsilon_r} + A_2)^{-A_3} \tag{58}$$

$$A_1 = \frac{30}{a}(4.9848 + 1.7841t - 7.319t^2 + 17.4513t^3) \tag{59}$$

$$A_2 = 0.20261 + 0.1819t - 0.3234t^2 - 0.1792t^3 \tag{60}$$

$$A_3 = 0.9968 + 0.005t + 0.0069t^2 - 0.1376t^3 \tag{61}$$

where $t = c/a$, the units of f_r and a are in GHz and mm, respectively, and the constraint conditions $4 \leq \varepsilon_r \leq 80$ and $0 \leq t \leq 0.6$ are imposed in (58). Here, we will consider the resonant frequency varying with the dielectric constant for the TE_{111} mode. The outer radius and inner radius of the DRA are fixed. The resultant resonant frequencies solved from (58) and the proposed CM theory are compared in Table II. We can see that the resonant frequencies for different dielectric constants agree well with each other. It again validates the accuracy of the proposed methods in predicting the resonant frequency of dielectric coated conducting bodies.

In summary, the proposed CM theory for dielectric coated conducting bodies is implemented in three typical examples. Numerical results are compared with those obtained from the widely used PEC CM theory and results in the published literature. It demonstrates that the resonant frequencies, characteristic fields of the dielectric coated conducting bodies, can be solved accurately by our proposed CM formulations. Moreover, the influence of the dielectric coatings on resonant frequencies is studied. Besides, we suggest that the mesh density should be within the range of $\lambda/15$–$\lambda/20$ (λ is the free space wavelength) to allow accurate descriptions of the modal behaviors of high order modes.

IV. CONCLUSION

Based on the EFIE-PMCHWT SIE, this paper develops the CM theory for dielectric coated conducting bodies. Through using Poynting's theorem, the eigenvalues are proved to have the same physical meaning as that in the conventional PEC CM theory. Numerical results are also presented to show the accuracy of the proposed CM formulation. It is expected that the proposed CM theory will be useful in the analysis and design of antenna involving dielectric coated conducting bodies.

It is necessary to emphasize that the CM theory in this paper is only suitable to coatings with real permittivity. Actually, development of CM formulation for lossy problem is still a challenging task. Even for lossy conducting bodies, the CM theory in [2] cannot clearly give meaningful CM analysis results as in PEC bodies (lossless). The main reason behind this difficulty is that it is difficult to separate the ohm loss from the stored and radiated power. It thus results in the difficulty in solving the true CMs through a simple generalized eigenvalue equation. Very recently, some practical postprocessing methods are proposed to remove nonphysical modes/internal modes appearing in lossy material problems [17]. We can employ these methods to carry out CM analysis of lossy EM problems.

In addition, the EFIE-PMCHWT SIE in this paper is obtained by invoking the equivalence principle in the interior and exterior region. It gives two SIEs and each SIE is only valid for their own region. The EFIE-PMCHWT is a combination of these SIEs. Therefore, the EFIE-PMCHWT is only suitable to fully dielectric coated PEC problems.

ACKNOWLEDGMENT

The authors would like to thank the anonymous reviewers for their valuable comments and suggestions, which have significantly improved the quality of this paper.

REFERENCES

[1] R. J. Garbacz, "Modal expansions for resonance scattering phenomena," *Proc. IEEE*, vol. 53, no. 8, pp. 856–864, Aug. 1965.
[2] R. F. Harrington and J. R. Mautz, "Theory of characteristic modes for conducting bodies," *IEEE Trans. Antennas Propag.*, vol. 19, no. 5, pp. 622–628, Sep. 1971.
[3] R. F. Harrington, J. R. Mautz, and Y. Chang, "Characteristic modes for dielectric and magnetic bodies," *IEEE Trans. Antennas Propag.*, vol. 20, no. 2, pp. 194–198, Mar. 1972.
[4] Y. Chang and R. F. Harrington, "A surface formulation for characteristic modes of material bodies," *IEEE Trans. Antennas Propag.*, vol. 25, no. 6, pp. 789–795, Nov. 1977.
[5] W. E. Howell and H. Uberall, "Complex frequency poles of radar scattering from coated conducting spheres," *IEEE Trans. Antennas Propag.*, vol. 32, no. 6, pp. 624–627, Jun. 1984.
[6] D. J. Taylor, A. K. Jordan, P. J. Moser, and H. Uberall, "Complex resonances of conducting spheres with lossy coatings," *IEEE Trans. Antennas Propag.*, vol. 38, no. 2, pp. 236–240, Feb. 1990.
[7] Y.-L. Geng and C.-W. Qiu, "Extended Mie theory for a gyrotropic-coated conducting sphere: An analytical approach," *IEEE Trans. Antennas Propag.*, vol. 59, no. 11, pp. 4364–4368, Nov. 2011.
[8] S. M. Rao, C.-C. Cha, R. L. Cravey, and D. L. Wilkes, "Electromagnetic scattering from arbitrary shaped conducting bodies coated with lossy materials of arbitrary thickness," *IEEE Trans. Antennas Propag.*, vol. 39, no. 5, pp. 627–631, May 1991.
[9] S. He and Z. Nie, "Accurate and fast calculation for dielectric-coated PEC surfaces with thin dielectric approximations," in *Proc. ICEAA*, Sydney, NSW, Australia, Sep. 2010, pp. 117–120.
[10] J.-J. Jin and V. V. Liepa, "Application of hybrid finite element method to electromagnetic scattering from coated cylinders," *IEEE Trans. Antennas Propag.*, vol. 36, no. 1, pp. 50–54, Jan. 1988.
[11] R. F. Harrington and J. R. Mautz, "Control of radar scattering by reactive loading," *IEEE Trans. Antennas Propag.*, vol. 20, no. 4, pp. 446–454, Jul. 1972.
[12] G. Angiulli, G. Amendola, and G. Di Massa, "Characteristic modes in multiple scattering by conducting cylinders of arbitrary shape," *Electromagnetics*, vol. 18, no. 6, pp. 593–612, 1998.
[13] G. Angiulli, G. Amendola, and G. D. Massa, "Application of characteristic modes to the analysis of scattering from microstrip antennas," *J. Electromagn. Waves Appl.*, vol. 14, no. 8, pp. 1063–1081, 2000.
[14] O. M. Bucci and G. D. Massa, "Use of characteristic modes in multiple-scattering problems," *J. Phys. D, Appl. Phys.*, vol. 28, no. 11, pp. 2235–2244, 1995.
[15] Y. Chen, "Alternative surface integral equation-based characteristic mode analysis of dielectric resonator antennas," *IET Microw., Antennas Propag.*, vol. 10, no. 2, pp. 193–201, Jan. 2016.
[16] F.-G. Hu and C.-F. Wang, "FE-BI formulations for characteristic modes," *IEEE Trans. Microw. Theory Techn.*, vol. 64, no. 5, pp. 1396–1401, May 2016.

[17] Z. T. Miers and B. K. Lau, "Computational analysis and verifications of characteristic modes in real materials," *IEEE Trans. Antennas Propag.*, vol. 64, no. 7, pp. 2595–2607, Jul. 2016.
[18] Y. Chen and C.-F. Wang, "Electrically small UAV antenna design using characteristic modes," *IEEE Trans. Antennas Propag.*, vol. 62, no. 2, pp. 535–545, Feb. 2014.
[19] Y. Chen and C. F. Wang, "HF band shipboard antenna design using characteristic modes," *IEEE Trans. Antennas Propag.*, vol. 63, no. 3, pp. 1004–1013, Mar. 2015.
[20] Y. Chen and C.-F. Wang, "Characteristic mode synthesis of omni-directional radiation patterns for electrically small UAV," in *Proc. IEEE Int. Symp. Antennas Propag.*, Vancouver, BC, Canada, Jul. 2015, pp. 1430–1431.
[21] Y. Chen and C.-F. Wang, "Synthesis of platform integrated antennas for reconfigurable radiation patterns using the theory of characteristic modes," in *Proc. Int. Symp. Antennas Propag. EM Theory*, Xi'an, China, Oct. 2012, pp. 281–285.
[22] M. Bouezzeddine and W. L. Schroeder, "Design of a wideband, tunable four-port MIMO antenna system with high isolation based on the theory of characteristic modes," *IEEE Trans. Antennas Propag.*, vol. 64, no. 7, pp. 2679–2688, Jul. 2016.
[23] H. Li, Z. T. Miers, and B. K. Lau, "Design of orthogonal MIMO handset antennas based on characteristic mode manipulation at frequency bands below 1 GHz," *IEEE Trans. Antennas Propag.*, vol. 62, no. 5, pp. 2756–2766, May 2014.
[24] Z. T. Miers, H. Li, and B. K. Lau, "Design of bandwidth enhanced and multiband MIMO antennas using characteristic modes," *IEEE Antennas Wireless Propag. Lett.*, vol. 12, pp. 1696–1699, 2013.
[25] M. Vrancken and G. A. E. Vandenbosch, "Characteristic modes for the multiple stacked aperture problem with application to the finite array analysis of flat plate slot array antennas," *Int. J. Electron. Commun.*, vol. 56, no. 6, pp. 411–415, Oct. 2002.
[26] M. Vrancken and G. A. E. Vandenbosch, "Characteristic aperture modes for the mutual coupling analysis in finite arrays of aperture-coupled antennas," *Int. J. Electron. Commun.*, vol. 56, no. 1, pp. 19–26, Jan. 2002.
[27] Y. Chen and C.-F. Wang, *Characteristic Modes: Theory and Applications in Antenna Engineering*. Hoboken, NJ, USA: Wiley, 2015, pp. 100–141.
[28] K. W. Leung, "Complex resonance and radiation of hemispherical dielectric-resonator antenna with a concentric conductor," *IEEE Trans. Microw. Theory Techn.*, vol. 49, no. 3, pp. 524–531, Mar. 2001.
[29] J. M. Jin, *Theory and Computation of Electromagnetic Fields*. Hoboken, NJ, USA: Wiley, 2010.
[30] D. Kajfez, A. W. Glisson, and J. James, "Computed modal field distributions of isolated dielectric resonators," *IEEE Trans. Microw. Theory Techn.*, vol. 32, no. 12, pp. 1609–1616, Dec. 1984.
[31] Y. Liu, S. Safavi-Naeini, S. K. Chaudhuri, and R. Sabry, "On the determination of resonant modes of dielectric objects using surface integral equations," *IEEE Trans. Antennas Propag.*, vol. 52, no. 4, pp. 1062–1069, Apr. 2004.

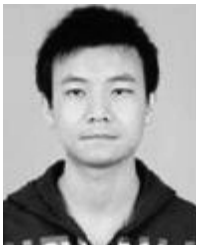

Liwen Guo was born in Shuozhou, Shanxi, China, in 1990. He received the B.Sc. degree in electromagnetics and wireless technology from the University of Electronic Science and Technology of China, Chengdu, China, in 2013, where he is currently pursuing the Ph.D. degree in electromagnetics and microwave technology.

His current research interests include theory and application of characteristic mode, integral equation, and antenna design.

Yikai Chen (M'12–SM'15) was born in Hangzhou, China, in 1984. He received the B.Eng. and Ph.D. degrees in electromagnetics and microwave technology from the University of Electronic Science and Technology of China (UESTC), Chengdu, China, in 2006 and 2011, respectively.

From 2011 to 2015, he was a Research Scientist with the Temasek Laboratories, National University of Singapore, Singapore. In 2015, he joined UESTC, as a Full Professor. He has authored or co-authored over 60 peer-reviewed papers and seven patents/patent disclosures. He has co-authored the book entitled *Characteristic Modes: Theory and Applications in Antenna Engineering* (John Wiley, 2015), and one book chapter to *Differential Evolution: Fundamentals and Applications in Electrical Engineering* (IEEE Wiley, 2009). His current research interests include antenna engineering, computational electromagnetics, and evolutionary optimization algorithms in electromagnetic engineering.

Dr. Chen is a member of the Applied Computational Electromagnetics Society (ACES). He was a recipient of the National Excellent Doctoral Dissertation Award of China in 2013. He was recognized as a Hundred Talents Program Professor of the UESTC, Thousand Talents Program Professor of China, and Thousand Talents Program Professor of Sichuan Province, China, in 2015, 2016, and 2017, respectively. He serves on the Editorial Board of the *Chinese Journal of Electronics*. He has also served on the review boards of many journals, including the IEEE TRANSACTIONS ON ANTENNAS AND PROPAGATION, and the IEEE ANTENNAS AND WIRELESS PROPAGATION LETTERS, and many international conferences as a TPC Member, a Session Organizer, and the Session Chair.

Shiwen Yang (M'00–SM'04) was born in Sichuan, China, in 1967. He received the B.S. degree in electronic science and technology from East China Normal University, Shanghai, China, in 1989, and the M.S. degree in electromagnetics and microwave technology and the Ph.D. degree in physical electronics from the University of Electronic Science and Technology of China (UESTC), Chengdu, China, in 1992 and 1998, respectively.

From 1994 to 1998, he was a Lecturer with the Institute of High Energy Electronics, UESTC. From 1998 to 2001, he was a Research Fellow with the School of Electrical and Electronic Engineering, Nanyang Technological University, Singapore. From 2002 to 2005, he was a Research Scientist with Temasek Laboratories, National University of Singapore, Singapore. Since 2005, he has been a Full Professor with the School of Electronic Engineering, UESTC. Since 2015, he has been a Chang-Jiang Professor nominated by the Ministry of Education of China. He has authored or co-authored over 200 technical papers. His current research interests include antennas, antennas arrays, optimization techniques, and computational electromagnetics.

Dr. Yang received the Foundation for China Distinguished Young Investigators presented by the National Science Foundation of China in 2011. He is the Chair of the IEEE AP-S/EMC-S Joint Chengdu Chapter, and served as an Editorial Board Member of *IJAP*, and *Chinese Journal of Electronics*.